REVIEW ARTICLE

Fifty years of nucleophilic substitution in the gas phase

Roland Wester

Institut für Ionenphysik und Angewandte Physik, Universität Innsbruck, Technikerstraße 25, 6020 Innsbruck, Austria

Email: roland.wester@uibk.ac.at

Abstract

Bimolecular nucleophilic substitution (S_N2) reactions have become a model system for the investigation of structure–reactivity relationships, stereochemistry, solvent influences, and detailed atomistic dynamics. In this review, the progress during five decades of experimental and theoretical research on gas phase S_N2 reactions is discussed. Many advancements of the employed methods have led to a tremendous increase in our understanding of the properties and the dynamics of these reactions. For reactions involving six atoms a quantitative agreement of the differential reactive scattering cross sections has already been achieved, in the future it is expected that even larger polyatomic reactions systems become tractable. Furthermore, studies with higher precision, improved reactant control, and a more accurate theoretical treatment of quantum effects are envisioned.

KEYWORDS

crossed-beam scattering, ion–molecule collisions, nucleophilic substitution, reaction kinetics, reaction mechanisms

1 | INTRODUCTION

Nucleophilic substitution reactions are one of the important classes of chemical reactions in organic synthesis. Being widely used in chemistry, the properties of substitution reactions have been investigated since the 19th century and they have played important roles in the development of an understanding how energetics, steric, or solvent effects affect chemical reactions. Here we focus on bimolecular nucleophilic substitution (S_N2) reactions, which occur in the simplest form at a saturated carbon atom and can be written as

$$X^- + CH_3Y \rightarrow Y^- + CH_3X. \tag{1}$$
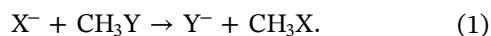
X and Y may be individual halogen atoms or various molecular compounds. In practical applications, one or more of the hydrogen atoms at the central carbon in Equation (1) are often replaced by side groups.

Back in 1896 Paul Walden investigated reactions of optically active halogen compounds. Studying chiral organic acids, specifically malic acid and chlorine or bromine substituted succinic acid, he found that upon reaction with silver oxide and phosphorous pentachloride one enantiomer could be transformed into the opposite enantiomer and back again (Walden, 1896), a process referred to as Walden cycle. In extensive work during the 1930s Hughes, Ingold, and coworkers (see Cowdrey et al., 1937; Hughes & Ingold, 1935) discussed first and second order nucleophilic substitution reactions, S_N1 and S_N2. They explained Walden's results by a steric inversion at the central carbon atom that occurs during S_N2 reactions and is now known as Walden inversion. In contrast, S_N1 reactions lead to a racemic mixture of products due to the formation of a detectable intermediate carbocation. This study shaped the notion that S_N2 reactions occur by concerted bond-formation and bond-cleavage following the approach of a nucleophile X^- towards the backside of the CH_3Y reactant. This description of S_N2 reactions has since found entry in the standard organic chemistry textbooks.

If second order nucleophilic substitution (S_N2) reactions, also referred to as nucleophilic displacement reactions, occur in a bimolecular collision process, they may be investigated in the absence of solvent molecules in gas phase experiments. This started 50 years ago (Bohme & Young, 1970) and led to numerous surprising discoveries until the present time (Xie & Hase, 2016). In the present review we discuss the results that have been obtained on gas phase S_N2 reactions during the last five decades. Different gas phase physical chemistry and chemical physics methods have been used since the first ion flow tube experiment in 1970. During this time, nucleophilic substitution reactions have possibly become the most intensely studied ion–molecule reaction. It is the aim of this review to present how the development and improvement of experimental and computational methods has allowed for more and more insight into these reactions. There certainly have been more publications on this topic than can be cited here, but we have tried to include reference to all important contributions that advanced the understanding of gas phase nucleophilic substitution reactions. Many reviews have discussed S_N2 reactions in the past, most notably the reviews by Laerdahl and Uggerud (2002), Mikosch et al. (2010), Xie et al. (2014), and most recently Uggerud (2017). Our reviews on crossed-beam reaction dynamics experiments also contained major parts on S_N2 reactions (Carrascosa, Meyer, & Wester, 2017; Meyer & Wester, 2017; Wester, 2014).

In Section 2 of this review the early experimental work on gas phase S_N2 reactions is discussed. The following section covers the mostly kinetics oriented focus of the work until about the year 2000 (Section 3). In the subsequent section (Section 4) spectroscopic studies of the reaction complex are discussed. This is followed by a section that presents the reaction dynamics research that started in the "zero years" of the present century (Section 5). Finally an outlook (Section 6) on probably several more decades of gas phase studies of S_N2 reactions is given.

2 | THE EARLY YEARS

Gas phase experiments on nucleophilic substitution reactions started fifty years ago with the work by Bohme and Young (1970). Using the flowing afterglow technique developed by Fehsenfeld and others, Bohme and Young measured the thermal reaction rate coefficients for a number of negative ion reactions with CH_3Cl. The focus of their work was on testing capture theory, which predicts ion–molecule reaction rates based on the long-range ion-induced dipole and ion-permanent dipole interaction. The former leads to the Langevin rate coefficient $k_L \propto \sqrt{\alpha/\mu}$, while the latter term is proportional to the

permanent dipole moment of the neutral (α is the polarizability of the neutral reactant and μ the reduced mass of the collision system). The experimental reaction efficiencies provided evidence to which extent dipole-locking occurs during a collision.

The Bohme group at York University continued to investigate the kinetics, equilibrium constants, and thermodynamics of S_N2 reactions of negative ions with CH_3Cl and CH_3F and also included combustion-relevant reactions, such as the reactions of C_2^- and CN^- with CH_4 or C_2H_2 (Schiff & Bohme, 1975). Later they moved to reactions of negative ions with silane, SiH_4, and compared this to reactions with methane (Payzant et al., 1976). While reactions of anions with methane were quite unreactive, reactions with silane showed large rate coefficients and many different reaction channels, which is attributed to the more favorable thermodynamics in reactions of SiH_4.

In parallel also first results for cationic nucleophilic displacement reactions in the gas phase were reported (Holtz et al., 1970). In this case the ion cyclotron resonance (ICR) technique was employed. This technique was also chosen by Brauman and coworkers, who investigated reactions of F^-, Cl^-, and CH_3S^- anions with CH_3Cl and CH_3Br (Brauman et al., 1974), which also allowed them to detect the neutral products (Lieder & Brauman, 1974). They measured changes in the reaction rate coefficients that were found to be small, but important, given the fact that barrierless ion–molecule reactions usually proceed with very similar capture rate coefficients. This led to the conclusion that an intermediate barrier is modifying nucleophilic displacement reactions.

Further experiments, where they obtained thermal rate coefficients for more than 30 different S_N2 reactions, led Brauman and coworkers to predict a double-well potential energy landscape for gas phase nucleophilic substitution reactions (Olmstead & Brauman, 1977) (see also Section 3.4). Two potential energy minima describe the entrance and exit channel complexes of reaction (1), $X^-(CH_3Y)$ and $(XCH_3)Y^-$, separated by an intermediate barrier that represents the transition state of the reaction (see Figure 1). The energy of this transition state is often found to be submerged with respect to the energy of the reactants, nevertheless it profoundly influences the reaction as a dynamical bottleneck where the density of states has a minimum.

3 | ION–MOLECULE KINETICS

For many years the research on gas phase nucleophilic substitution reactions focused on reaction kinetics and thermodynamics. Theoretically, a growing number of quantum chemical calculations have been performed and
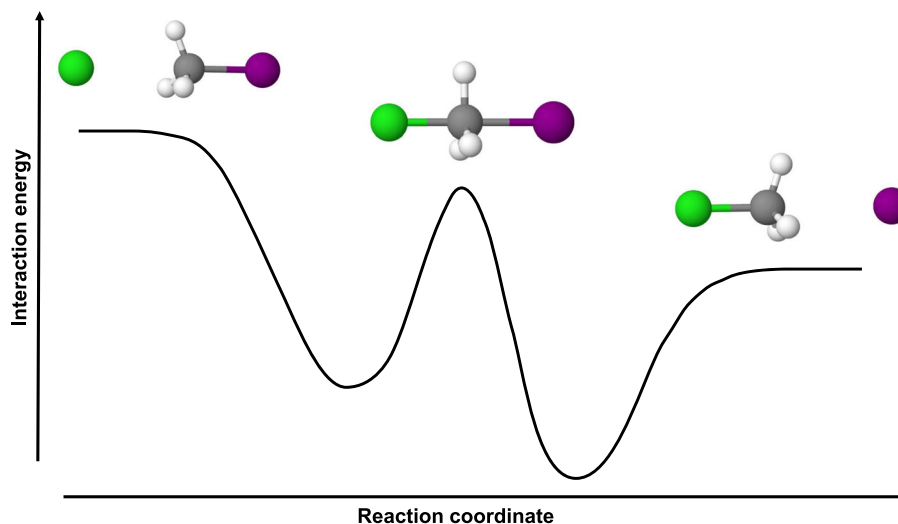
FIGURE 1 Double-well potential of a typical gas phase S_N2 reaction (see reaction 1) [Color figure can be viewed at wileyonlinelibrary.com]

statistical modeling has been used to calculate rate coefficients. Experimentally, a range of techniques, such as ion flow tubes, ion cyclotron resonance mass spectrometry, high pressure mass spectrometry and, later, guided ion beam techniques were used to obtain kinetic data, in particular temperature- and collision-energy-dependent reaction rate coefficients, cross sections, and equilibrium constants. With these techniques, more detailed insight in the the reaction efficiencies, the energetics along the reaction coordinate, or the role of solvent molecules, in comparison with reactions in solution, has been obtained.

3.1 | Theoretical modeling

Quantum chemical investigations of nucleophilic substitution reactions started in the mid 1970s. Early calculations at the self-consistent field (SCF) level investigated possible different reactions pathways and calculated transition state energies, such as for the frontside and backside attack in the $F^- + CH_3F$ system (Schlegel et al., 1977). In further theoretical work different factors that influence barrier heights of S_N2 reactions were studied, in particular the ionization energy of the nucleophile and the electron affinity of the neutral molecule (Shaik & Pross, 1982), or the influence of substituents at the central carbon atom on the transition state energy (Wolfe et al., 1982). It was also calculated, in this case for the $C^- + CH_3Cl$ reaction, that the binding energies of the reaction complexes and the height of the barrier are strongly influenced by solvent effects (Chandrasekhar et al., 1984, 1985), which explains the strong suppression of S_N2 reactivity in solution phase compared to the gas phase.

Using post-Hartree Fock methods the reaction profile of the $H^- + CH_3F$ reaction as well as the vibrational frequencies of the reaction complex at different stationary points was calculated by Zahradnik and coworkers (Havlas et al., 1988). Based on these quantum chemical calculations the group then performed detailed RRKM calculations to determine the absolute reaction rate coefficient for this reaction (Merkel et al., 1988). To achieve this they modeled the reaction as a three-step process, capture into the entrance channel complex, passage of the transition state, and dissociation of the exit channel complex. They compared several quantum chemistry theories and basis sets and were able to reach good agreement with previous experimental results (Tanaka et al., 1976).

Shortly after, Vande Linde and Hase studied the symmetric S_N2 reaction $Cl^- + CH_3Cl$ in a series of articles (Vande Linde & Hase, 1989, 1990a, 1990b, 1990c). They were able to construct a global potential energy surface for this reaction (Vande Linde & Hase, 1990a) and used this to run classical trajectories to calculate the atomistic reaction dynamics and obtain absolute cross sections as a function of relative energy (see Figure 2). This allowed them to identify a direct reaction mechanism for this substitution reaction (Vande Linde & Hase, 1989). Furthermore, they found that this mechanism can be promoted by exciting several quanta of the C-Cl stretch vibration in CH_3Cl, while exciting the CH_3 deformation did not lead to product formation (Vande Linde & Hase, 1989). In the final paragraph of their first article Vande Linde and Hase state: "It is hoped that the work presented here will lead to experimental investigations of a direct mechanism for $X^- + CH_3Y \rightarrow XCH_3 + Y^-$ nucleophilic substitution."
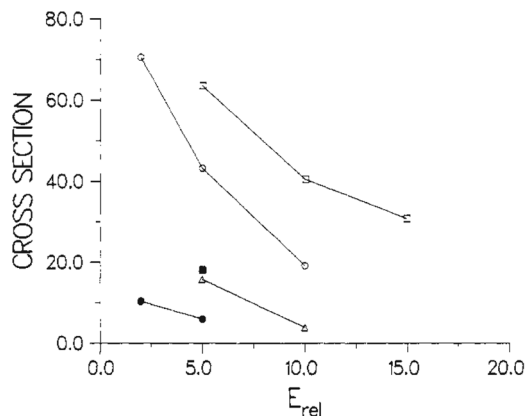
FIGURE 2 Absolute reactive cross section ($\mathring{A}^2$) as a function of the relative collision energy (kcal/mol) for the $Cl^- + CH_3Cl$ reaction. Open symbols are calculated for $T_{rot} = 0$ K and full symbols for $T_{rot} = 300$ K, triangles are for four quanta of excitation in the C-Cl stretch vibration, circles for six quanta and squares for eight quanta. Reprinted with permission from Vande Linde and Hase (1989). Copyright (1989) American Chemical Society

(Vande Linde & Hase, 1989). This in fact became true almost twenty years later, when a direct reaction mechanism was observed experimentally in the $Cl^- + CH_3I$ reaction (Mikosch, Trippel, et al., 2008) (see Section 5).

In their next article, Vande Linde and Hase found non-RRKM behavior for the above substitution reaction. Their calculated decomposition lifetimes of the $Cl^-(CH_3Cl)$ complex showed a multiexponential decay. Further analysis revealed that vibrational coupling in the complex is weak, which prohibits the application of RRKM calculations since fast intramolecular vibrational energy redistribution (IVR) among all internal vibrational degrees of freedom is a fundamental assumption in RRKM theory. The application of trajectory simulations to nucleophilic substitution reactions and the discovery of non-RRKM behavior stimulated the study of these reactions for many years. More of these simulations will be discussed in Section 5.1 below.

For the same reaction, $Cl^- + CH_3Cl$, the role of water as solvent molecules was calculated by Tucker and Truhlar both with respect to the reaction energetics and the expected rate coefficients (Tucker & Truhlar, 1990). The variational transition state theory calculations yielded a strong suppression of the reaction rate coefficient by several orders of magnitude when one or two water molecules are attached to the Cl^- nucleophile. This trend follows a corresponding increase of the intermediate reaction barrier upon microsolvation. In a second publication they also investigated the kinetic isotope effect that occurs when hydrogen atoms are replaced by deuterium (Zhao et al., 1991).

Higher level quantum chemistry calculations have been carried out by Glukhovtsev et al. in a series of articles (Glukhovtsev et al., 1995; Glukhovtsev, Pross, & Radom, 1996; Glukhovtsev, Pross, Schlegel, et al., 1996). In their first article they studied the identity reactions of X^- with CH_3X for the four halides X = F, Cl, Br, and I. They obtained C_{3v} geometries for intermediate reaction complexes, the complexation energies, intermediate barrier heights, and charge distributions (Glukhovtsev et al., 1995). They then studied all nonidentity reactions $X^- + CH_3Y$ (X,Y = F, Cl, Br, I) at the same level of theory and analyzed the results using Marcus theory (Glukhovtsev, Pross, & Radom, 1996).

Further steps towards understanding chemical reactivity based on quantum chemical calculations have been presented by Bickelhaupt, who used density functional theory (DFT) and analyzed the Kohn-Sham molecular orbitals to decompose the relevant energies of stationary states along the reaction coordinate (Bickelhaupt, 1999), which was also used for comparison with the energetics in solution. This study was later extended to a range of 64 S_N2 reactions, comparing several different DFT functionals (Swart et al., 2007).

3.2 | Flow tube experiments on bimolecular rate coefficients

Experimental activity on the kinetics of substitution reactions continued to involve the use of the flow tube technique (Viggiano & Morris, 1996). Several improvements were developed that made more detailed experimental investigations possible: The addition of a reactant ion mass filter in the selected ion flow tube (SIFT) instrument allowed one to study only the ion of interest in the flow tube. The addition of a drift tube, where ions are slighly accelerated, allowed one to separate internal reactant temperature from average collision energy in the center of mass frame. And finally temperature-variable setups yielded further control of the internal and translational energies of the reactants in ion-molecule reactions.

Using a sensitive SIFT instrument, the identity S_N2 reaction $Cl^- + CH_3Cl$ was studied over a collision energy range of 0.04–2 eV (Barlow et al., 1988). With SIFT experiments also the role of solvents, which influence substitution reactions in the liquid phase significantly, moved into focus. Reactant ions were clustered to a selected number of chosen solvent molecules before they were brought to reaction in the flow or drift tube. Such micro-solvation experiments were carried out for a range of ions and solvents. Reactions of F^- and Cl^- attached to water, methanol, ethanol, aceton, formic acid, and acetic

acid have been studied by Bohme and Raksit (1985). Experiments on the effect of water attached to OH^- on reactions with methyl chloride were discussed by Hierl et al., who used flow tube and ion beam techniques to study reaction probabilities up to several electronvolt of translational energy (Hierl et al., 1988) and were also able to observe proton transfer in competition with S_N2 products. All these experiments showed an overall suppression of the reaction rate coefficients with increasing number of solvent molecules. This agrees with theoretical findings, as discussed in the previous section and the known lower reaction rate coefficients for substitution reactions in the liquid phase.

The development of temperature-variable flow tubes allowed experiments to move beyond reaction kinetics at room temperature and provided insight into the temperature-dependence of substitution kinetics. Using drift tube measurements over the temperature range of 200–560 K, Viggiano et al. showed that the $Cl^- + CH_3Br$ reaction rate coefficient is strongly dependent on the relative translational energy. At the same time it is insensitive to the internal temperature of the molecular reactant (Viggiano et al., 1992). This was clear experimental evidence that the main assumption of statistical theories, the fast randomization of energy in the reaction complex, is violated.

S_N2 reaction kinetics have also been studied at ambient pressure using a kinetic ion mobility mass spectrometer developed by Giles and Grimsrud (1992). Using this instrument rate coefficients for the exothermic reactions of Cl^- with methyl, ethyl, and n-butyl bromide have been measured for temperatures of 35–150° C (Knighton et al., 1993). In case of the methyl chloride reactions, the authors observed collisional stabilization. By analysis of the measured rates, the energy of the submerged reaction barrier with respect to the energy of the reactant was extracted (Knighton et al., 1993).

With the CRESU (a French acronym for Cinétique de Réaction en Ecouliement Supersonique) technique, ion–molecule reactions can be studied under low-temperature conditions. In the uniform expansion that forms after a precisely designed Laval nozzle constant high densities and temperatures are reached, which allows for the equilibration of all translational and internal degrees of freedom. The CRESU technique was employed by Le Garrec et al. (1997) to study the S_N2 reaction $Cl^- + CH_3Br$ from 180 K down to 23 K. Their results showed a strong increase of the rate coefficient with decreasing temperature (open circles in Figure 3). At 23 K the rate is only about a factor of two smaller than the capture rate, while a 30-fold reduction is reached at 180 K. This trend extends up to 500 K when combining the CRESU data with previous rate coefficient
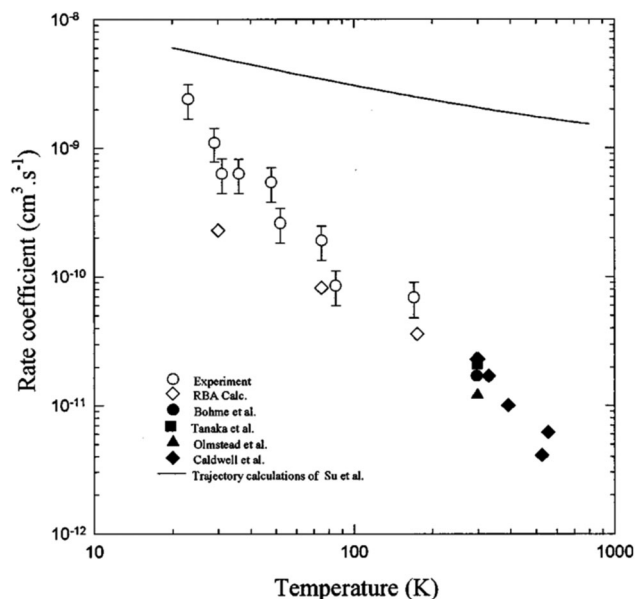

FIGURE 3 Open symbols: Measured and calculated absolute rate constant for the substitution reaction $Cl^- + CH_3Br$ (Le Garrec et al., 1997). Full symbols are data from Bohme and Raksit (1985), Caldwell et al. (1984), Olmstead and Brauman (1977), and Tanaka et al. (1976) shown for comparison. Solid line: Calculation from Su and Chesnavich (1982). Reprinted with permission from Le Garrec et al. (1997)

measurements. Overall the rate decreases by a factor of 400 between 23 and 500 K. Quantum scattering calculations for different values of the total angular momentum have been performed and, after proper Boltzmann averaging, compared to the measurement, where a good agreement is found (see Figure 3). The strong decrease, not known in other ion–molecule reactions, is essentially attributed to the coupling of the intermolecular vibrational modes in the entrance channel with the density of states at the intermediate barrier for the reaction, which is just slightly submerged with respect to the energy of the reactants (Le Garrec et al., 1997).

Significant effort has been put into understanding if S_N2 reactivity is enhanced if the anionic nucleophile carries a lone pair of electrons adjacent to the attacking atom, referred to as α-effect. Early studies indicated that this effect, which is important in solution phase, was not found in the gas phase when comparing the reactivity of OH^- with HOO^- (DePuy et al., 1983). However, more recently it could be shown that the α-effect is in fact an intrinsic property of gas phase S_N2 reactions (Garver et al., 2011; Thomsen et al., 2013).

Besides the predominantly studied substitution reactions with anionic nucleophiles, also cationic S_N2 reactions have been investigated. As an example, Kretschmer et al. (2012) present the formation of $CH_3NH_3^+$ following a Walden inversion in a collision of $M(CH_3)^+$ with NH_3,

where M = Zn, Cd, or Hg. The measured reaction probabilites increased from about 2% for Cd up to about 20% for Hg, but remained far below the long-range capture limit similar to what has been found for anionic S_N2 reactions.

3.3 | Kinetic energy release measurements

A set of experiments on the kinetic energy release distribution of transient S_N2 complexes have been performed by Graul and Bowers (1991). In their first work $Cl^-(CH_3Br)$ complexes were produced and mass-selected. Then the unimolecular decay of these complexes was observed and the relative kinetic energy of the products was recorded. On the time-scale of the experiment of tens of microseconds only the reactive product ion Br^- was observed and not the decay back to reactant anion Cl^-. The measured kinetic energy release distribution for $Br^- + CH_3Cl$ shows an average energy release of 30 ± 10 meV.

It was concluded that the produced metastable complexes carried between 1 and 2 eV of internal energy, more than the complex binding energy of about 0.5 eV, and decay with lifetimes below the observation time window of microseconds. With this input phase space theory (PST) calculations were performed to model the kinetic energy release following statistical randomization of the internal energy. The resulting PST distribution yielded more than twice the product kinetic energy than experimentally observed. This nonstatistical energy partitioning is clear evidence for the fact that this nucleophilic substitution reaction can not be correctly described by statistical models. Instead, the authors speculate that the excess energy may be stored in the C-Cl stretch and/or the CH_3 umbrella vibration (Graul & Bowers, 1994).

In further work similar results have been found for the $Cl^-(CH_3I)$ and $Br^-(CH_3I)$ complexes for reactions towards I products, as well as for their deuterated variants (Graul & Bowers, 1994). The results were compared both with a statistical model and with a variant of that model where part of the energy was assumed to be locked-up in vibrational excitation of the neutral reaction product CH_3Cl or CH_3I. Using that assumption the statistical model could be brought to agreement with the measured kinetic energy release distributions (Graul et al., 1998). Also larger reaction complexes, such as $Cl^-(CH_3CH_2I)$ or $F^-(C_6H_5OCH_3)$ were found to show qualitatively similar nonstatistical behavior, but with slightly smaller discrepancies between the measured distributions and the statistical model (Graul et al., 1998).

3.4 | Ion cyclotron resonance measurements

The ion cyclotron resonance (ICR) technique has been continued to be used by Brauman and coworkers for a range of studies after their pioneering work (Olmstead & Brauman, 1977). Reactant ions were trapped in the ICR trap and exposed to a constant background gas density of the neutral reactant. The rate of disappearance of the reactant ion or the appearance of product ions can be measured, either by resonant excitation or by ion ejection. It has been tested that the reactant ions thermalize in the trap and that therefore reliable thermal rate coefficients are obtained. These measured rate coefficients were described by a step-wise reaction model and involving statistical rate calculations for the individual steps: capture in the entrance channel complex, passage of the transition state to the exit channel complex, dissociation of the exit channel complex (see e.g., Chabinyc et al., 1998).

In later work, ICR studies of the identity S_N2 reactions of Y^- with CH_2CNY or $C_6H_5CH_2Y$ (Y = Cl and Br) have been performed (Wladkowski & Brauman, 1993). Thermal rate coefficients have been measured at a temperature estimated to be 350 K and binding energies of the reaction complexes have been determined from measured equilibrium constants. Using statistical theories the energetics of the potential energy surface have been determined and analyzed using Marcus theory (Wladkowski & Brauman, 1993). Gas phase S_N2 reactions of even larger neutral reactants have been studied by Craig et al. They investigated identity reactions of Cl^- with $Cl(CH_2)_nX$, where the n-alkyl chlorides are substituted, for example, with X = CN, Cl, or OH (Craig & Brauman, 1996, 1999).

Further work on identity reactions allowed Regan et al. to show that steric effects are less important for thermal S_N2 reactions in the gas phase than they are in solution. Also, it is shown that the strong increase of the S_N2 barrier height when moving from gas phase to solution phase is due to the strong interaction of the solvent molecules with the nucleophile and the leaving group (Regan et al., 2002).

Cationic reactions have also been investigated with the ICR technique, in particular by the Uggerud group. They studied, for example, reactions of different oxonium ions with ammonia observing a range of products (Bache-Andreassen & Uggerud, 2000, 2003).

3.5 | Guided ion beam studies of absolute cross sections

Higher collision energies than in heated flow or drift tube experiments are achieved with the guided ion beam technique (Armentrout, 2000). With this approach,

absolute reaction cross sections have been measured by Ervin and coworkers for several nucleophilic substitution reactions. Given the higher collision energies that are accessible with this technique, up to many electronvolts, several endoergic reaction pathways could be studied as well. DeTuri et al. investigated the symmetric S_N2 reaction $Cl^- + CH_3Cl \rightarrow ClCH_3 + Cl^-$ (DeTuri et al., 1997) by isotopic labeling. They found a threshold energy of 470 ± 160 meV for this reaction, in substantial disagreement with a previous determination of about 2 eV using a drift tube experiment (Barlow et al., 1988). The theoretically estimated barrier height at the transition state for the S_N2 backside attack amounts to only around 120 meV, which shows that additional dynamical constraints must be at work in this symmetric reaction.

In further guided ion beam-experiments the exothermic S_N2 reaction $F^- + CH_3Cl$ and its endothermic reverse reaction $Cl^- + CH_3F$ have been studied (Angel & Ervin, 2001; Angel et al., 2002). The technique allowed for the measurement of absolute reaction cross sections over a dynamic range from more than 10^2 Å^2 down to 5×10^{-4} Å^2 (see Figure 4). Several different product channels were studied besides nucleophilic substitution, including exoergic proton transfer reaction and dihalide (FCl^-) formation channels.

The exothermic S_N2 reaction was found to be most efficient at low relative collision energies. Its cross section decreases rapidly in the energy range of 0.1 to 2 eV. This is attributed to more impulsive collisions at higher collision energy, where a reorientation of the neutral reactant to the incoming ion becomes less and less probable (Angel & Ervin, 2001). This explanation invokes a fast direct collision and is therefore different from the one given for the rate decrease observed at lower collision energies in the CRESU measurements of Le Garrec et al. (1997) discussed above. There it was attributed to the decreased probability for coupling of the vibrational states in the entrance channel with the density of states at the transition state.

For the endothermic S_N2 reaction an energy threshold is observed, which is determined to be about 1.9 eV. This value is larger than the calculated reaction endothermicity by about 0.5 eV and shows, similar to the symmetric S_N2 reaction $Cl^- + CH_3Cl$ that was discussed above, that dynamical constraints can suppress the reactivity in these reactions even above threshold. Similar results have been obtained for the endoergic reaction of I^- with CH_3Cl and CH_3Br (Angel & Ervin, 2004).

In a guided ion beam study of the $Cl^- + CH_3Br$ reaction not only absolute reaction cross sections, but also scattering angle-dependent dynamical information was inferred (Angel & Ervin, 2003).
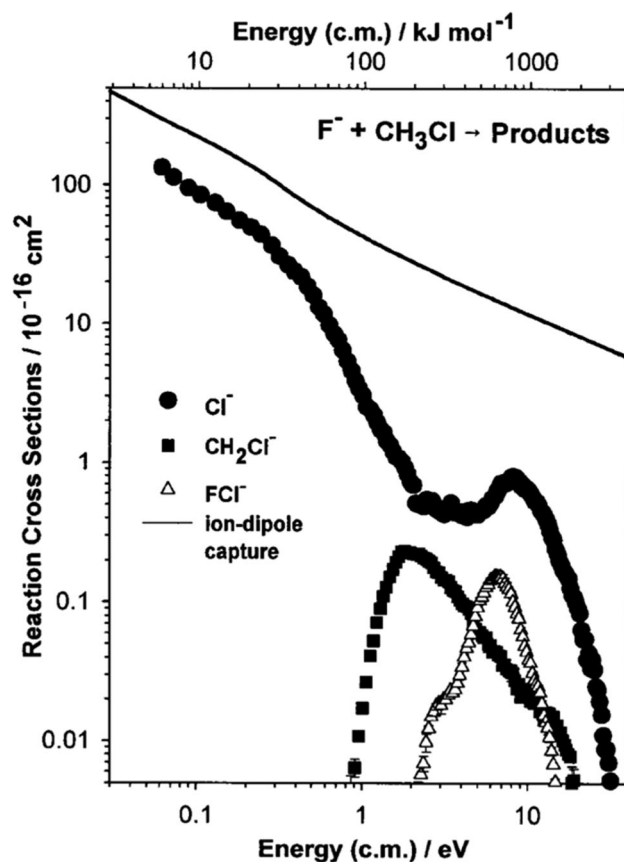

FIGURE 4 Measured reaction cross section for the $F^- + CH_3Cl$ reaction as a function of collision energy in the center of mass frame. Reprinted with permission from Angel and Ervin (2001). Copyright (2001) American Chemical Society

3.6 | High pressure mass spectrometry and ternary rates in ion traps

High pressure mass spectrometry (HPMS) has become another powerful tool to study ion–molecule reactions, in particular their thermochemistry (Kebarle, 2000). McMahon and coworkers have used this to study a range of nucleophilic substitution reactions with particular focus on their equilibrium constants and the thermodynamics of their entrance channel wells and barrier heights. In C. Li et al. (1996) they studied the symmetric S_N2 reaction $Cl^- + CH_3Cl$ and the nonsymmetric reactions of Cl^- with methyl-, ethyl, iso-propyl and t-butyl bromide. Furthermore, they analyzed the three-body association rate for the entrance channel complex $Cl^-(CH_3Cl)$ of the symmetric S_N2 reaction and extracted its lifetime with respect to decay back to reactants (C. Li et al., 1996). Their value of about 12 ps agreed very well with trajectory simulations by Vande Linde and Hase on the same system (Vande Linde & Hase, 1990c).
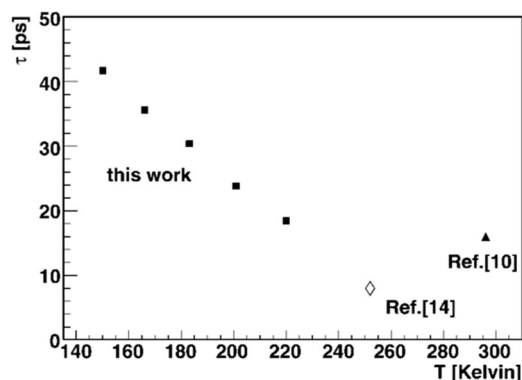
FIGURE 5 Lifetimes of the entrance channel complex Cl⁻(CH₃Cl) of the corresponding symmetric S_N2 reaction, measured by high pressure mass spectrometry at room temperature (C. Li et al., 1996) (solid triangle) and as a function of temperature in a cryogenic radiofrequency ion trap (Mikosch, Otto, et al., 2008) (solid squares). The experimental values agree well with the trajectory simulation result (Vande Linde & Hase, 1990c) (open diamond). Reprinted with permission from Mikosch, Otto, et al. (2008). Copyright (2008) American Chemical Society

In further work the HPMS technique was used to study the thermochemistry of reactions of ions that are micro-solvated with several neutral solvent molecules (methanol, acetonitrile, acetone, and difluoroethane) (Bogdanov & McMahon, 2005) and of reactions with fluorine-substituted neutrals, specifically trifluoromethyl halides (Bogdanov & McMahon, 2006). Both frontside and backside reaction complexes have been found, but it was shown that the S_N2 reaction with trifluoromethyl halides proceeds preferentially via backside attack and Walden inversion (Figure 5).

Complementary to the high pressure studies, reaction kinetics and three-body collisions can also been studied in a low-temperature radiofrequency ion trap (Wester, 2009). There, lower reactant gas densities and instead longer interaction times are available. In a study of the symmetric S_N2 reaction complex Cl⁻(CH₃Cl) (Mikosch, Otto, et al., 2008), ternary collisions of Cl⁻ with CH₃Cl and different third bodies were investigated at temperatures between 150 and 220 K. The ternary rate coefficient has been determined and a much stronger inverse temperature dependence has been found than expected from a statistical model. From these data the lifetime of the transient S_N2 complex Cl⁻(CH₃Cl) has been derived as a function of temperature. The lifetime increases significantly upon decreasing temperature, whereas at 220 K a good agreement is reached both with the HPMS lifetime discussed above (C. Li et al., 1996) and the trajectory calculation (Vande Linde & Hase, 1990c).

4 | SPECTROSCOPY OF S_N2 REACTION COMPLEXES

Several spectroscopic approaches have attempted to shed light on the intermediate reaction complexes of nucleophilic substitution reactions. Negative ion photoelectron spectroscopy has been applied to several S_N2 reaction complexes by Cyr et al. They studied in particular the pre-reaction complexes I⁻(CH₃I) (Cyr et al., 1994, 1992, 1993). The photoelectron spectra revealed the red shift of the two photoelectron peaks of bare I⁻ due to the binding of CH₃I as well as a vibrational fine structure that could be assigned to a progression of the C-I stretching vibration. Shortly after, zero-electron kinetic energy spectroscopy could reveal several low-frequency bands due to intermolecular vibrations in the pre-reaction complex (Arnold et al., 1995). Recently the I⁻·ICF₃ was studied using 2D photoelectron spectroscopy and compared to the earlier work. There the complex was shown to represent the frontside attack with I⁻ bound to the iodine atom of CF₃I (Mensa-Bonsu et al., 2019).

Using infrared spectroscopy, Johnson and coworkers investigated the photo-induced dissociation of the entrance and exit channel complexes of the Cl⁻ + CH₃Br reaction following infrared CH stretch vibrational excitation (Ayotte et al., 1999). Using argon-tagging predissociation spectroscopy, absorption was detected in the Cl⁻(CH₃Br) complex, shifted to the blue with respect to the symmetric and asymmetric CH stretch excitations in bare CH₃Br due to the interaction with the chlorine anion. Subsequently, product Br⁻ formation was observed following this excitation for the entrance channel complex, which shows that the Walden transition state has been passed. In contrast, for the exit channel complex Br⁻(CH₃Cl) no product formation was observed, because in this case the photon energy is insufficient to dissociate the complex. Shortly after, the dissociation of the entrance channel complex Cl⁻(CH₃Br) into CH₃Cl and Br⁻ has also been detected using black-body induced dissociation and using a continuous-wave mid-infrared CO₂ laser(Tonner & McMahon, 2000).

Femtosecond time-resolved photoelectron spectroscopy has been used to access the dissociation of an S_N2 reaction complex in the time domain (Wester et al., 2003). The entrance channel complex I⁻(CH₃I) has been prepared by photodissociation of the I₂⁻ bond in I₂⁻(CH₃I) precursor anions with a femtosecond pump pulse. The time evolution of the I⁻(CH₃I) complex has then been followed using a second femtosecond pulse that led to photodetachment. The resulting photoelectron kinetic energy spectra have been measured as a function of the pump–probe delay time. The observed decay back to to the I⁻ + CH₃I reactants was found to occur with a bi-exponential decay on two time scales, about 0.75 and

10 ps. The occurance of this bi-exponential decay was attributed to nonstatistical vibrational energy redistribution in the complex (Wester et al., 2003).

5 | ION–MOLECULE REACTION DYNAMICS

The following section describes the experimental and theoretical achievements that have been made towards understanding the reaction dynamics underlying nucleophilic substitution. Using energy- and angle-differential reactive scattering experiments and elaborate direct dynamics and quasiclassical trajectory calculations, insight into reaction mechanisms, product energy partitioning, and dependence on initial rovibrational excitation has been obtained. Also quantum reactive scattering calculations are being performed, but they are mostly still restricted to reduced dimensions.

5.1 | Trajectory simulations of substitution dynamics

Numerous chemical dynamics simulations have been carried out for substitution reactions using trajectory calculations. Several Pionieering studies were already discussed in Section 3.1 above, see also Hase (1994). With these simulations, reaction probabilities and opacity functions $P(b)$ are determined as a function of the clasical impact parameters b, typically up to the maximum impact parameter given by Langevin or capture theory and as a function of collision energy. Integrating this function yields the energy-dependent cross section and by thermal averaging the temperature-dependent reaction rate coefficient. By closely inspecting the trajectories different reaction pathways and mechanisms can be investigated. Furthermore, scattering angle distributions and probability distributions for internal rovibrational or translational energies can be extracted in a straightforward manner. Quantum zero-point vibrational energies can be introduced by adding initial internal energy to the molecular degrees of freedom and product rovibrational state analysis may be achieved by appropriate binning techniques.

Mostly, trajectory simulations make use of a potential energy surface (PES) to obtain the interatomic forces. However, for high-dimensional scattering problems that involve six or more atoms, such as S_N2 reactions, full-dimensional global potential energy surfaces are demanding to calculate. To avoid calculating a PES, direct dynamics calculations have been developed, in particular by Hase and coworkers (Lourderaj et al., 2014). Here, the potential energy gradients are calculated by solving the electronic structure problem on-the-fly, while integrating a trajectory. This makes the trajectory calculation computationally costly, but does not require prior knowledge of the PES and may also be used more easily for higher scattering energies. In addition, this method calculates the potential energy exactly at the required intermolecular geometries.

For the substitution reaction $Cl^- + CH_3Cl$ both PES-based (Mann & Hase, 1998) and direct dynamics (G. S. Li & Hase, 1999) trajectory simulations have been performed to gain more insight into this symmetric reaction. This study confirmed the backside attack mechanism, no frontside reactions were observed. Furthermore, it was found that the reaction proceeds via backward scattering in a rebound-type mechanism, that is, the product ion velocity points in the same direction as the reactant ion velocity. Only a small fraction of the trajectories react via an indirect complex-forming mechanism. This is discussed to occur, because the coupling of the translational collision energy to the internal degrees of freedom of the reaction complex is weak, which is clear evidence for nonstatistical reaction dynamics.

In the reaction $OH^- + CH_3F$ even more striking nonstatistical dynamics were discovered (Sun et al., 2002). Using direct dynamics trajectory calculations the chemical dynamics of this reaction have been investigated and it was found that the deep minimum in the exit region of the potential energy surface is only seldomly explored during the reaction. Most of the trajectories (about 90%) did not follow the internal reaction coordinate (IRC) pathway and avoided this minimum. This is in contrast to the underlying assumption of statistical models that a reaction proceeds by transitions from stationary state to stationary state with reaction rates for each step that only depend on the number or density of states at these configurations and the intermediate transition states. Sun et al. (2002) discussed their results in the context of IVR, which was found to be very inefficient in this reaction.

Further direct dynamics simulations have been carried out by Tachikawa on several substitution reactions (Tachikawa, 2006; Tachikawa & Igarashi, 1999, 2006), including reactions of singly hydrated anions, $F^-(H_2O)$ and $OH^-(H_2O)$. This study supported the notion of a direct reaction and also found that most of the energy available to the products is partitioned into translational energy (Tachikawa & Igarashi, 1999). Despite the low number of computed trajectories also branching ratio for the different product channels of the micro-hydrated reactions could be extracted (Tachikawa, 2006) and hydrated product ions were found to constitute only a minor channel in the reaction of $OH^-(H_2O)$ with CH_3Cl.

ab initio molecular dynamics of the exothermic S_N2 reaction $Cl^- + CH_3Br$ have also been reported by Schettino and coworkers (Raugei et al., 1999) including the investigation of microsolvation effects (Raugei et al., 2001).

Stimulated by the advent of crossed-beam reactive scattering experiments, the reactions of Cl^-, F^-, OH^-, and $OH^-(H_2O)$ with CH_3I have been extensively studied by Hase and coworkers using direct dynamics simulations (Mikosch, Trippel, et al., 2008; Xie et al., 2015, 2013; Zhang & Hase, 2010; Zhang et al., 2009, 2013, 2010). In the next section these results are discussed together with the experimental findings. For the reaction $F^- + CH_3I$, where some deviation between experiment and theory was observed, thorough tests of the dependence of the results on the underlying electronic structure calculation were performed (Sun, Davda, et al., 2015; Sun, Xie, et al., 2015).

Within the last decade the development of full-dimensional potential energy surfaces for S_N2 reactions has made great progress (Czakó et al., 2021). Czakó and coworkers developed global PESs for several substitution reactions including the $F^- + CH_3Cl$ (Szabó et al., 2013) and $F^- + CH_3I$ reactions (Olasz et al., 2017). With a PES available, typically two orders of magnitude more trajectories can be calculated than possible with direct dynamics, more than 500,000 trajectories were calculated for the reaction $F^- + CH_3Cl$ (Stei et al., 2016). Thus, the statistical significance of comparisons between experiment and theory has improved significantly, as shown in the good agreement with experimental differential scattering data for this reaction (Stei et al., 2016) (see Section 5.2).

With their accurate trajectory simulations for the $F^- + CH_3Cl$ reaction (Szabó et al., 2013), Czakó and coworkers discovered a novel and unexpected double-inversion mechanism for nucleophilic substitution (Szabó & Czakó, 2015) and, in collaboration with experiment, realized the importance of the frontside attack for the reaction dynamics of S_N2 reactions (Stei et al., 2016; Szabó et al., 2017). Further results on mode-specific S_N2 dynamics are discussed below together with the experimental results.

5.2 | Mechanisms of substitution reactions by crossed-beam scattering

Detailed insight into the dynamics of elementary reactions in the gas phase has been obtained from crossed-beam scattering experiments. Such experiments have been pursued for decades on neutral-neutral reactive collisions, such as the well-known $F + H_2$ reaction (Herschbach, 1987; Lee et al., 1969; Neumark, Wodtke, Robinson, Hayden, & Lee, 1985; Neumark, Wodtke, Robinson, Hayden, Shobatake, et al., 1985). Using ion imaging detectors in crossed-beam experiments a significant improvement in detection sensitivity could be made and at the same time fewer systematic errors affect the measured differential scattering cross section (Heck & Chandler, 1995; Kitsopoulos et al., 1993). With the advent of velocity map imaging (Eppink & Parker, 1997) a versatile electrode configuration with significantly enhanced ion velocity resolution became available and quickly spread to many laboratories around the world. The first attempt to use this for ion–molecule reaction studies were undertaken by Weishaar and coworkers for reactions of cobalt cations with propane and isobutane (Reichert et al., 2002a, 2002b).

In our group we have developed a crossed-beam velocity map imaging spectrometer for ion–molecule reactions (Mikosch et al., 2006; Trippel et al., 2009; Wester, 2014), which we have employed for a number of cation- and anion-reactions in the past 15 years (Carrascosa, Meyer, & Wester, 2017; Meyer & Wester, 2017). In the mean time ion–molecule crossed-beam imaging spectrometers have also been developed by Farrar and coworkers (Pei & Farrar, 2012; Pei et al., 2015) and Tian and coworkers (Hu et al., 2018) and applied to several reactions of atomic cations. Another imaging setup for ion–molecule crossed-beam studies has been presented by Gao and coworkers (Zhang et al., 2021).

A particular focus of our work has been on negative ion nucleophilic substitution reactions. Here, in an experiment on the $Cl^- + CH_3I$ reaction, we were able to observe for the first time the direct rebound mechanism (Mikosch, Trippel, et al., 2008). Its signature is direct back-scattering of the leaving anion I^- with respect to the direction of the incoming CH_3I, with high translational energy close to the total available energy. Hence, little energy is deposited in internal degrees of freedom of the CH_3Cl product (Xie et al., 2019). This reaction mechanism proceeds along a colinear reaction coordinate with C_{3v} symmetry and involves the inversion of the CH_3 group, as derived for bimolecular nucleophilic substitution (S_N2) reactions by Ingold and coworkers in the 1930s (Cowdrey et al., 1937; Hughes & Ingold, 1935). In addition to the direct rebound mechanism, we observed an indirect complex-mediated reaction mechanism. At high collision energy we discovered another indirect reaction mechanism. Based on direct dynamics simulations by Hase and coworkers, we could attribute this to a novel roundabout mechanism (Mikosch, Trippel, et al., 2008).

Overall, we have studied substitution reactions of Cl^-, F^-, OH^- and CN^- nucleophiles with methyl iodide and methyl chloride reactants (Carrascosa et al., 2015;

Mikosch et al., 2013; Otto et al., 2013; Otto, Brox, et al., 2012; Otto, Xie, et al., 2012; Stei et al., 2016). Striking differences have been observed for F^- and OH^- nucleophiles. Their stronger interaction and the smaller volume of their electron density distribution compared to Cl^- and CN^- allows them to approach the neutral reactant much closer and form hydrogen-bonded entrance channel complexes in addition to the more common reactant complexes with C_{3v} symmetry (Mikosch et al., 2013). This leads to an enhancement of indirect complex-mediated reactive scattering as well as a forward-scattering stripping mechanism, where the product ion moves roughly along the same direction as the incoming CH_3I. A detailed summary of the different reaction mechanisms found is given in Xie et al. (2014).

Images of the differential cross section for the reaction of F^- with CH_3Cl are shown in Figure 6 for two different collision energies (Stei et al., 2016). Two different features in the images are visible, a low product velocity distribution at the center of the image and a crescent-shaped feature on the right side of the images. The first feature represents reactions occuring by an indirect complex-mediated reaction mechanism, while the second feature is characteristic of the direct rebound mechanism.

Similar to the guided-ion-beam experiments, the crossed-beam experiments allow for larger collision energies up to several electronvolts. Moving to these higher energies, differential scattering cross sections for the endothermic reaction channels of the $F^- + CH_3I$ reaction, proton transfer to CH_2I^-, dihalide FI^- formation and also formation of FHI^- could be studied (Carrascosa et al., 2016).

5.3 | Influence of water molecules on the reaction dynamics

In further work, we investigated the reactive scattering of OH^- anions attached to one or two water water molecules with CH_3I (Otto, Brox, et al., 2012). To prepare the anion clusters with only a small, well-controlled amount of internal excitation, they were trapped in a radiofrequency octupole trap for about 20 ms before being brought to collision with the molecular beam of CH_3I. The trap was cooled to about 100 K, which is sufficient to freeze out almost all vibrational excitation in the negative ions (Otto, Xie, et al., 2012).

For bare OH^- anions reacting with CH_3I three different reaction mechanisms were observed in the differential scattering cross sections for 0.5–2 eV collision energy: indirect complex-mediated dynamics, forward and sideways stripping, and direct rebound dynamics (Otto, Brox, et al., 2012). The differential scattering images then changed substantially when one or two water molecules bind to the OH^- reactant. The forward scattered products are not observable when either one or two water molecules are attached. Instead, for the $OH^-(H_2O)$ cluster the back-scattered I^- products become the most prominent reaction channel, which corresponds to the rebound mechanism. For two water molecules only isotropic scattering with low product velocities is observed.

The enhancement of the direct rebound mechanisms for one water attached to the OH^- nucleophile was explained by structure calculations, which showed that the water molecule provides a steric guidance of the nucleophile towards the CH_3 group of methyl iodide in the reaction's entrance channel complex (Otto, Brox, et al., 2012). Detailed direct dynamics simulations by Xie et al. (2015) confirmed this and found good overall agreement with the experimental scattering data.

Micro-hydration effects have recently also been studied in reactions $F^-(H_2O)$ and $Cl^-(H_2O)$ reacting with CH_3I (Bastian, Michaelsen, Li, et al., 2020). The dominant product in these reactions is bare I^- and not the thermodynamically favored $I^-(H_2O)$, in good agreement with trajectory simulations by Zhang and coworkers. Similar findings have been made earlier for
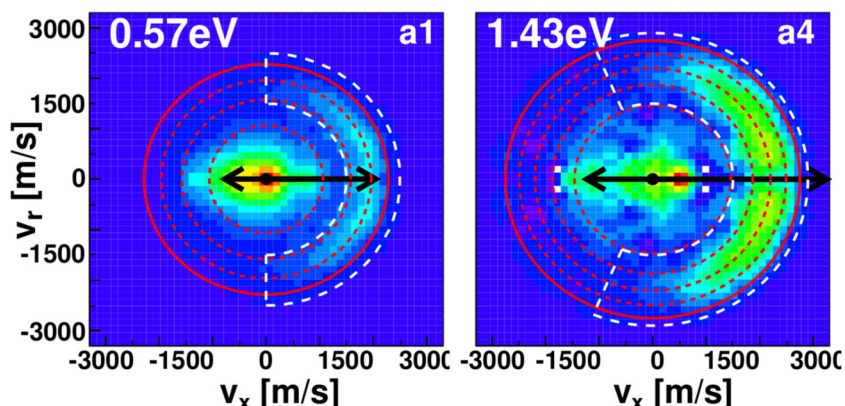

FIGURE 6 Differential scattering images for the S_N2 reaction $F^- + CH_3Cl$ at two different collision energies. Reprinted with permission from Stei et al. (2016) [Color figure can be viewed at wileyonlinelibrary.com]

microhydrated OH⁻ reactions (Otto et al., 2013). Both I⁻ and I⁻(H₂O) products form mostly via an indirect mechanism with isotropic and small product velocities. Compared to unsolvated reactions, the indirect fraction is significantly increased due to the water molecule. At 2.6 eV the scattering images for F⁻(H₂O) also show the signature of the direct rebound mechanism (Bastian, Michaelsen, Li, et al., 2020).

In the microhydrated reaction of Cl⁻(H₂O) very small product velocities were found to be fully suppressed, in contrast to other studied indirect reaction mechanisms (Bastian, Michaelsen, Li, et al., 2020; Bastian et al., 2021). A very similar feature was found in ligand exchange reaction pathway of singly hydrated halides F⁻(H₂O) + CH₃I → [FCH₃I]⁻ + H₂O (Bastian, Michaelsen, Ončák, et al., 2020). This suppression could be explained by the fragmentation of a transient or product reaction complex, which occurs when the internal energy is large enough to initiate unimolecular dissociation before the complex can be detected (Bastian et al., 2021).

5.4 | Controlling S$_N$2 reactions with initial vibrational excitation

In a set of experiments the influence of vibrational excitation of the CH-stretching mode on the S$_N$2 reaction F⁻ + CH₃I has been investigated (Michaelsen, Bastian, Ayasli, et al., 2020; Michaelsen, Bastian, Strübin, et al., 2020; Stei et al., 2018). Overall, CH stretching vibrations had been considered spectator modes that do not affect the reaction, when it occurs via backside attack by the direct rebound mechanism. This was supported by QCT calculations (Wang et al., 2016), while earlier quantum scattering calculations had predicted different cross sections for vibrationally excited reactants in the Cl⁻ + CH₃Br reaction (Hennig & Schmatz, 2007). In experiments where the symmetric CH stretching vibration in CH₃I was excited in a few percent of the reactants right before the interaction with the anionic nucleophile occured, we were able to show that the excitation does not change the reactivity of this S$_N$2 reaction (Stei et al., 2018). Experimental proof that scattering indeed occured with excited reactants was provided by the strong influence of the vibrational excitation on the proton transfer reaction pathway, which leads to CH₂I⁻ formation and was measured together with the S$_N$2 product I⁻.

In further work on the F⁻ + CH₃I reaction, which included different collision energies, we could identify that vibrational enhancement may indeed enhance S$_N$2 reactivity when occuring at a collision energy of 2.5 eV (Michaelsen, Bastian, Ayasli, et al., 2020). A similar trend

has been found in QCT simulations (Olasz and Czakó, 2018). In contrast, the proton transfer reaction is strongly enhanced at low collision energies, and much less affected at high collision energies. For halide abstraction, which leads to the formation of FI⁻ and FHI⁻ products, the reactivity was found to be suppressed. The spectator mode behavior for S$_N$2 reactions and the enhancement of proton transfer rections is in agreement with the sudden vector projection (SVP) model (Guo & Jiang, 2014; Jiang & Guo, 2013), which provides an extension of the Polanyi rules (Polanyi, 1972) to polyatomic reactions.

Vibrational excitation not only influences the overall reactivity of different reaction pathways, it can also directly affect the reaction dynamics. This was found for the proton transfer reaction in F⁻ + CH₃I collisions where indirect complex-mediated dynamics dominate at low collision energies (0.7 eV), whereas a shift to a direct stripping mechanism is observed at high collision energies (2.3 eV) (Michaelsen, Bastian, Strübin, et al., 2020).

5.5 | Quantum scattering calculations of substitution reactions

Full quantum scattering calculations of chemical reactions are necessary to properly account for zero-point energies and include interference, resonance, and tunneling effects (Clary, 1998). However, they are computationally much more demanding than trajectory simulations. For many years only three-atom reactions, such as F + H₂ Qiu et al. (2006), were calculated in this way. For larger systems, reduced-dimensionality quantum scattering calculations are being pursued.

Clary was the first to perform quantum scattering calculations for an S$_N$2 reaction (Le Garrec et al., 1997) (see Section 3.2). Later Schmatz and coworkers studied the identity and nonidentity S$_N$2 reactions of Cl⁻ with CH₃Cl and CH₃Br by including up to 4 of 12 internal degrees of freedom in their time-independent quantum scattering calculations (Hennig & Schmatz, 2004, 2005, 2007; Schmatz, 2004). In this way, vibrational state-dependent reaction cross sections were obtained. By selecting different degrees of freedom for the quantum calculations, specifically rotational instead of vibrational degrees of freedom, differential scattering cross sections (Hennig & Schmatz, 2012) and the dependence of the cross section on the initial rotational angular momentum could be calculated (Hennig & Schmatz, 2016).

Recently, a six-dimensional quantum scattering calculation has been achieved by Wang et al. (2016), who studied the F⁻ + CH₃Cl reaction based on the model of Palma and Clary (2000). These calculations supported

the indirect mechanism at low and the direct mechanism at higher collision energies. They also analyzed the vibrational state-dependence of the reaction cross section, as discussed in Section 5.4 above. Furthermore, time-dependent wavepacket calculations have also been carried out, again in reduced dimensions, and the product internal energy has been computed, which were found to compare qualitatively well with experiment (Kowalewski et al., 2014).

6 | SUMMARY AND OUTLOOK

Interest in gas phase nucleophilic substitution reactions has been driven by the ability to investigate the reactivity of this important class of reactions without the influence of solvent molecules (Bohme & Young, 1970). During the last 50 years, experimental and theoretical studies have provided a wealth of insight into their intrinsic dynamics. Reaction probabilities have been extracted from rate coefficient and cross section measurements by comparing measured data with capture cross sections that are determined purely by the long-range interaction. Equilibrium constants yielded exothermicities and binding energies of reaction complexes. From these data the view of a reaction resulted that proceeds across a double-well potential energy landscape with an intermediate, often submerged, reaction barrier (Olmstead & Brauman, 1977). Using this view, calculations based on statistical theories allowed for quantitative comparison with measured rate coefficients. The ability to add solvent molecules to the reactant ion one by one has been widely used to investigate how the reaction is influenced (Chabinyc et al., 1998). The statistical picture, however, was soon challenged by various experimental and theoretical evidence, such as reaction probabilities that do not change with vibrational excitation (Viggiano et al., 1992), product energy partitioning that does not couple to certain vibrational modes of a transient reaction complex (Graul & Bowers, 1994), or reactions that avoids trapping in its intermediate reaction complexes (Sun et al., 2002).

In the last 20 years the research focus has shifted to obtain a better and more quantitative understanding of the atomistic dynamics of nucleophilic substitution reactions. The advent of ion–molecule crossed-beam reactive scattering experiments (Mikosch, Trippel, et al., 2008) and the improvement of trajectory simulations, most recently on accurate full-dimensional potential energy surfaces (Czakó et al., 2021), has made this possible. Energy- and angle-differential cross sections have been obtained, and remarkable agreement has been achieved between experiment and theory (Stei et al., 2016). A range of reaction mechanisms have been disentangled, including the direct rebound mechanism via backside attack, the complex-mediated mechanism, the direct stripping mechanism, or the roundabout mechanism (Mikosch, Trippel, et al., 2008; Xie et al., 2014).

The question is what is ahead? S_N2 reactions have continued to surprise, for example, with the recent discovery of a novel double-inversion mechanism (Szabó & Czakó, 2015). One of the most important questions for chemical reactions in general, what is the role of quantum mechanical dynamics, is nowhere near to being answered, despite the fact that zero-point energy and tunneling through the intermediate barrier may impact the dynamics significantly. The study of isotope effects, using deuterated reactants, may shed some light on this. Also, precise comparison of differential cross sections from experiment and theory have shown some remaining deviations. Further precision crossed-beam studies will be carried out to clarify if these deviations point to nonclassical dynamics. With better understanding comes the aim to control reaction outcomes of S_N2 reactions. Vibrational state-selected reaction experiments have already shown that reaction cross sections can be influenced (Michaelsen, Bastian, Ayasli, et al., 2020). It will be interesting, and challenging, to extend this study to the lower lying vibrational modes of the CH_3 umbrella and to the C-Y vibration.

A range of studies have already focused on the reaction dynamics of micro-hydrated reactants. In applications, however, reactions are not only used in water, but in a range of solvents. Comparing the influence of different solvents on the atomistic dynamics in micro-solvation experiments is still in its infancy. Furthermore, when substituting the hydrogen atoms in reaction (1) by alkyl chains, different and in general even richer reaction dynamics become possible.

With two or more carbon centers, base-induced elimination can occur and competes with nucleophilic substitution. A review of E2 reaction studies over the last fifty years would fill a second article. Research on the competition between these and S_N2 reactions, which lead to the same ionic product, started early using kinetic isotope effects or secondary reactions to distinguish the two pathways (Gronert et al., 1991; Wladkowski & Brauman, 1992). Later dianion reactants were employed for this purpose (Gronert, 2003). More recently, crossed-beam imaging has allowed us to study the direct competition between S_N2 and E2 reactions (Carrascosa et al., 2018; Carrascosa, Meyer, Zhang, et al., 2017; Meyer et al., 2019). In the future this technique may also be applied to aromatic substitution (S_NAr) reactions (Sharma et al., 2020). Thus, gas phase studies can be expected to continue to improve our understanding of chemical reactions for many years to come.

ACKNOWLEDGMENTS

REFERENCES

Angel LA, Ervin KM. 2001. Dynamics of the gas-phase reactions of fluoride ions with chloromethane. *J. Phys. Chem. A. 105*(16): 4042-4051.

Angel LA, Ervin KM. 2003. Gas-phase S_N2 and bromine abstraction reactions of chloride ion with bromomethane: Reaction cross sections and energy disposal into products. *J. Am. Chem. Soc. 125*: 1014-1027.

Angel LA, Ervin KM. 2004. Gas-phase reactions of the iodide ion with chloromethane and bromomethane: Competition between nucleophilic displacement and halogen abstraction. *J. Phys. Chem. A. 108*: 9827-9833.

Angel LA, Garcia SP, Ervin KM. 2002. Dynamics of the gas-phase reactions of chloride ion with fluoromethane: High excess translational activation energy for an endothermic S_N2 reaction. *J. Am. Chem. Soc. 124*: 336.

Armentrout PB. 2000. Kinetic energy dependence of ion-molecule reactions: Guided ion beams and threshold measurements. *Int. J. Mass Spectrom. 200*: 219-41.

Arnold CC, Neumark DM, Cyr DM, Johnson MA. 1995. Negative-ion zero electron kinetic-energy spectroscopy of I^-·CH_3I. *J. Phys. Chem. 99*(6): 1633-1636.

Ayotte P, Kim J, Kelley JA, Nielsen SB, Johnson MA. 1999. Photoactivation of the Cl^- + CH_3Br S_N2 reaction via rotationally resolved C-H stretch excitation of the Cl^-·CH_3Br entrance channel complex. *J. Am. Chem. Soc. 121*(29): 6950-6951.

Bache-Andreassen L, Uggerud E. 2000. Mechanisms of reactions between ammonia and methylene oxonium ions: Immonium ion formation versus transfer of the oxygen substituent. *Int. J. Mass Spectrom. 195*: 171-184.

Bache-Andreassen L, Uggerud E. 2003. Trends in alkyl substituent effects on nucleophilic reactions of carbonyl compounds: Gas phase reactions between ammonia and ($R^1R^2COCH_3^+$) oxonium ions. *Org. Biomol. Chem. 1*: 705-713.

Barlow SE, Doren JMV, Bierbaum VM. 1988. The gas-phase displacement reaction of chloride ion with methyl chloride as a function of kinetic energy. *J. Am. Chem. Soc. 110*(21): 7240-7242.

Bastian B, Michaelsen T, Li L, Ončák M, Meyer J, Zhang DH, Wester R. 2020. Imaging reaction dynamics of $F^-(H_2O)$ and $Cl^-(H_2O)$ with CH_3I. *J. Phys. Chem. A 124*(10): 1929-1939.

Bastian B, Michaelsen T, Ončák M, Meyer J, Wester R. 2020. $F^-(H_2O)$ + CH_3I ligand exchange reaction dynamics. *Chin. J. Chem. Phys. 33*(2): 210.

Bastian B, Michaelsen T, Ončák M, Meyer J, Wester R. 2021. Suppression of low product kinetic energies in reactions of FHO^- and $Cl^-(H_2O)$ with CH_3I. *Int. J. Mass Spectrom. 462*: 116526.

Bickelhaupt FM. 1999. Understanding reactivity with Kohn-Sham molecular orbital theory: E2 − S_N2 mechanistic spectrum and other concepts. *J. Comput. Chem. 20*(1): 114-128.

Bogdanov B, McMahon TB. 2005. Thermochemistry and structures of solvated S_N2 complexes and transition states in the gas phase: experiment and theory. *Int. J. Mass Spectrom. 241*(2-3): 205-223. (Special Issue in Honour of William L. Hase).

Bogdanov B, McMahon TB. 2006. Gas phase S_N2 reactions of halide ions with trifluoromethyl halides: Front- and back-side attack vs. complex formation. *J. Phys. Chem. A. 110*: 1350-1363.

Bohme DK, Raksit AB. 1985. Gas-phase measurements of the influence of stepwise solvation on the kinetics of S_N2 reactions of solvated F^- with CH_3Cl and CH_3Br and of solvated Cl^- with CH_3Br. *Can. J. Chem. 63*(11): 3007-3011.

Bohme DK, Young LB. 1970. Kinetic studies of reactions of oxide, hydroxide, alkoxide, phenyl, and benzylic anions with methyl chloride in gas phase at 22.5 degrees. *J. Am. Chem. Soc. 92*(25): 7354.

Brauman JI, Olmstead WN, Lieder CA. 1974. Gas-phase nucleophilic displacement-reactions. *J. Am. Chem. Soc. 96*(12): 4030-4031.

Caldwell G, Magnera TF, Kebarle P. 1984. S_N2 reactions in the gas phase. temperature dependence of the rate constants and energies of the transition states. comparison with solution. *J. Am. Chem. Soc. 106*: 959.

Carrascosa E, Bawart M, Stei M, Linden F, Carelli F, Meyer J, Geppert WD, Gianturco FA, and Wester R. 2015. Nucleophilic substitution with two reactive centers: The CN^- + CH_3I case. *J. Chem. Phys. 143*(18): 184309.

Carrascosa E, Meyer J, Michaelsen T, Stei M, Wester R. 2018. Conservation of direct dynamics in sterically hindered S_N2/E2 reactions. *Chem. Sci. 9*(3): 693-701.

Carrascosa E, Meyer J, Wester R. 2017. Imaging the dynamics of ion-molecule reactions. *Chem. Soc. Rev. 46*(24): 7498-7516.

Carrascosa E, Meyer J, Zhang J, Stei M, Michaelsen T, Hase WL, Yang L, Wester R. 2017. Imaging dynamic fingerprints of competing E2 and S_N2 reactions. *Nat. Commun. 8*(1): 25.

Carrascosa E, Michaelsen T, Stei M, Bastian B, Meyer J, Mikosch J, Wester R. 2016. Imaging proton transfer and dihalide formation pathways in reactions of F^- + CH_3I. *J. Phys. Chem. A 120*(27): 4711-4719.

Chabinyc ML, Craig SL, Regan CK, Brauman JI. 1998. Gas-phase ionic reactions: Dynamics and mechanism of nucleophilic displacements. *Science 279*(5358): 1882-1886.

Chandrasekhar J, Smith SF, Jorgensen WL. 1984. S_N2 reaction profiles in the gas phase and aqueous solution. *J. Am. Chem. Soc. 106*(10): 3049-3050.

Chandrasekhar J, Smith SF, Jorgensen WL. 1985. Theoretical-examination of the S_N2 reaction involving chloride-ion and methyl-chloride in the gas-phase and aqueous-solution. *J. Am. Chem. Soc. 107*(1): 154-163.

Clary DC. 1998. Quantum theory of chemical reaction dynamics. *Science 279*: 1879.

Cowdrey WA, Hughes ED, Ingold CK, Masterman S, Scott AD. 1937. Reaction kinetics and the walden inversion. part vi. relation of steric orientation to mechanism in substitutions involving halogen atoms and simple or substituted hydroxyl groups. *J. Chem. Soc.* 2: 1252-1271.

Craig SL, Brauman JI. 1996. Intramolecular microsolvation of thermoneutral gas-phase S_N2 reactions. *J. Am. Chem. Soc.* 118: 6786-6787.

Craig SL, Brauman JI. 1999. Intramolecular microsolvation of S_N2 transition states. *J. Am. Chem. Soc.* 121(28): 6690-6699.

Cyr DM, Bailey CG, Serxner D, Scarton MG, Johnson MA. 1994. The charge-transfer excited-state of the $I^- \cdot CH_3I$ S_N2 reaction intermediate - photoinduced intracluster dissociative attachment. *J. Chem. Phys.* 101: 10507-10520.

Cyr DM, Bishea GA, Scarton MG, Johnson MA. 1992. Observation of charge-transfer excited-states in the $I^- \cdot CH_3I$, $I^- \cdot CH_3Br$, and $I^- \cdot CH_2Br_2$ S_N2 reaction intermediates using photofragmentation and photoelectron spectroscopies. *J. Chem. Phys.* 97(8): 5911-5914.

Cyr DM, Scarton MG, Johnson MA. 1993. Photoelectron-spectroscopy of the gas-phase s_n2 reaction intermediates $I^- \cdot CH_3I$ and $I^- \cdot CD_3I$—distortion of the CH_3I at the ion-dipole complex. *J. Chem. Phys.* 99(6): 4869-4872.

Czakó, G., Györi T, Papp D, Tajti V, Tasi DA. 2021. First-principles reaction dynamics beyond six-atom systems. *J. Phys. Chem. A.*

DePuy, CH, Della EW, Filley J, Grabowski JJ, Bierbaum VM. 1983. Absence of an alpha-effect in the gas-phase nucleophilic reactions of HOO^-. *J. Am. Chem. Soc.* 105(8): 2481-2482.

DeTuri VF, Hintz PA, Ervin KM. 1997. Translational activation of the S_N2 nucleophilic displacement reactions $Cl^- + CH_3Cl(CD_3Cl) \rightarrow ClCH_3(ClCD_3) + Cl^-$: A guided ion beam study. *J. Phys. Chem. A.* 101(34): 5969-5986.

Eppink ATJB, Parker DH. 1997. Velocity map imaging of ions and electrons using electrostatic lenses: Application in photoelectron and photofragment ion imaging of molecular oxygen. *Rev. Sci. Instrum.* 68(9): 3477-3484.

Garver JM, Gronert S, Bierbaum VM. 2011. Experimental validation of the α-effect in the gas phase. *J. Am. Chem. Soc.* 133(35): 13894-13897.

Giles K, Grimsrud EP. 1992. The kinetic ion mobility mass-spectrometer - measurements of ion molecule reaction-rate constants at atmospheric-pressure. *J. Phys. Chem.* 96: 6680-6687.

Glukhovtsev MN, Addy P, Radom L. 1995. Gas-phase identity S_N2 reactions of halide anions with methyl halides: A high-level computational study. *J. Am. Chem. Soc.* 117(7): 2024-2032.

Glukhovtsev MN, Pross A, Radom L. 1996. Gas-phase non-identity S_N2 reactions of halide anions with methyl halides: A high-level computational study. *J. Am. Chem. Soc.* 118: 6273-6284.

Glukhovtsev MN, Pross A, Schlegel HB, Bach RD, Radom L. 1996. Gas-phase identity S_N2 reactions of halide anions and methyl halides with retention of configuration. *J. Am. Chem. Soc.* 118: 11258.

Graul ST, Bowers MT. 1991. The nonstatistical dissociation dynamics of $Cl^-(CH_3Br)$: Evidence for vibrational excitation in the products of gas-phase S_N2 reactions. *J. Am. Chem. Soc.* 113: 9696.

Graul ST, Bowers MT. 1994. Vibrational excitation in products of nucleophilic substitution: The dissociation of metastable $X^-(CH_3Y)$ in the gas phase. *J. Am. Chem. Soc.* 116: 3875-3883.

Graul ST, Carpenter CJ, Bushnell JE, van Koppen PAM, Bowers MT. 1998. Internal excitation in the products of nucleophilic substitution from the dissociation of metastable ion complexes. *J. Am. Chem. Soc.* 120: 6785.

Gronert S. 2003. Gas phase studies of the competition between substitution and elimination reactions. *Acc. Chem. Res.* 36(11): 848-857.

Gronert S, DePuy CH, Bierbaum VM. 1991. Deuterium isotope effects in gas-phase reactions of alkyl halides: distinguishing E2 and S_N2 pathways. *J. Am. Chem. Soc.* 113(10): 4009-4010.

Guo H, Jiang B. 2014. The sudden vector projection model for reactivity: Mode specificity and bond selectivity made simple. *Acc. Chem. Res.* 47(12): 3679-3685.

Hase WL. 1994. Simulations of gas-phase chemical reactions: Applications to S_N2 nucleophilic substitution. *Science.* 266(5187): 998-1002.

Havlas Z, Merkel A, Kalcher J, Janoschek R, Zahradnik R. 1988. Abinitio quantum chemical study of the S_N2 reaction, $CH_3F + H^- \rightarrow CH_4 + F^-$, in the gas-phase. *Chem. Phys.* 127(1-3): 53-63.

Heck AJR, Chandler DW. 1995. Imaging techniques for the study of chemical reaction dynamics. *Annu. Rev. Phys. Chem.* 46(1): 335-372.

Hennig C, Schmatz S. 2004. State-selected dynamics of the complex-forming bimolecular reaction $Cl^- + CH_3Cl \rightarrow ClCH_3 + Cl^-$: A four-dimensional quantum scattering study. *J. Chem. Phys.* 121: 220.

Hennig C, Schmatz S. 2005. Reduced-dimensionality calculation of reaction cross sections and rate constant for the complex-forming gas-phase S_N2 reaction $Cl^- + CH_3Cl \rightarrow ClCH_3 + Cl^-$. *Phys. Chem. Chem. Phys.* 7: 1552.

Hennig C, Schmatz S. 2007. Spectator modes in reaction dynamics revisited: Reaction cross sections and rate constant for $Cl^- + CH_3Br \rightarrow ClCH_3 + Br^-$ from quantum scattering. *Chem. Phys. Lett.* 446(4-6): 250-255.

Hennig C, Schmatz S. 2012. Differential reaction cross sections from rotationally resolved quantum scattering calculations: application to gas-phase S_N2 reactions. *Phys. Chem. Chem. Phys.* 14(37): 12982-12991.

Hennig C, Schmatz S. 2016. Reaction cross sections and tthermal rate constant for $Cl^- + CH_3Br \rightarrow ClCH_3 + Br^-$ from J-dependent quantum scattering calculations. *Phys. Chem. Chem. Phys.* 18: 19668.

Herschbach DR. 1987. Molecular dynamics of elementary chemical reactions (nobel lecture). *Angew. Chem., Int. Ed.* 26: 1221-1243.

Hierl PM, Ahrens AF, Henchman MJ, Viggiano AA, Paulson JF, Clary DC. 1988. Chemistry as a function of solvation number. solvated-ion reactions in the gas phase and comparison with solution. *Faraday Discuss. Chem. Soc.* 85(0): 37-51.

Holtz D, Beaucham JL, Woodgate SD. 1970. Nucleophilic displacement reactions in gas phase. *J. Am. Chem. Soc.* 92(25): 7484.

Hu J, Wu C-X, Ma Y, Tian SX. 2018. Collision-energy dependence of the ion-molecule charge exchange reaction $Ar^+ + NO$. *J. Phys. Chem. A.* 122(47): 9171-9176.

Hughes ED, Ingold CK. 1935. Mechanism of substitution at a saturated carbon atom. part iv. a discussion of constitutional and solvent effects on the mechanism, kinetics, velocity, and orientation of substitution. *J. Chem. Soc.* 1: 244-255.

Jiang B, Guo H. 2013. Relative efficacy of vibrational vs. translational excitation in promoting atom-diatom reactivity: Rigorous examination of polanyi's rules and proposition of sudden vector projection (SVP) model. *J. Chem. Phys.* 138(23): 234104.

Kebarle P. 2000. Gas phase ion thermochemistry based on ion-equilibria from the ionosphere to the reactive centers of enzymes. *Int. J. Mass Spectrom.* 200: 313-330.

Kitsopoulos TN, Buntine MA, Baldwin DP, Zare RN, Chandler DW. 1993. Reaction product imaging: The H + D_2 reaction. *Science* 260: 1605.

Knighton WB, Bognar JA, Oconnor PM, Grimsrud EP. 1993. Gas-phase S_N2 reactions of chloride-ion with alkyl bromides at atmospheric-pressure - temperature-dependence of the rate constants and energies of the transition-states. *J. Am. Chem. Soc.* 115: 12079-12084.

Kowalewski M, Mikosch J, Wester R, de Vivie-Riedle R. 2014. Nucleophilic substitution dynamics: Comparing wave packet calculations with experiment. *J. Phys. Chem. A* 118(26): 4661-9.

Kretschmer R, Schlangen M, Kaupp M, Schwarz H. 2012. Neutral metal atoms acting as a leaving group in gas-phase S_N2 reactions: $M(CH_3)^+ + NH_3 \rightarrow CH_3NH_3^+ + M(M = Zn, Cd, Hg)$. *Organometallics.* 31: 3816-3824.

Laerdahl JK, Uggerud E. 2002. Gas phase nucleophilic substitution. *Int. J. Mass Spectrom.* 214(3): 277-314.

LeGarrec JL, Rowe BR, Queffelec JL, Mitchell JBA, Clary DC. 1997. Temperature dependence of the rate constant for the $Cl^- + CH_3Br$ reaction down to 23 K. *J. Chem. Phys.* 107: 1021-1024.

Lee YT, McDonald JD, LeBreton PR, Herschbach DR. 1969. Molecular beam reactive scattering apparatus with electron bombardment detector. *Rev. Sci. Instrum.* 40: 1402-1408.

Li C, Ross P, Szulejko JE, McMahon TB. 1996. High-pressure mass spectrometric investigations of the potential energy surfaces of gas-phase S_N2 reactions. *J. Am. Chem. Soc.* 118: 9360.

Li GS, Hase WL. 1999. Ab initio direct dynamics trajectory study of the $Cl^- + CH_3Cl$ S_N2 reaction at high reagent translational energy. *J. Am. Chem. Soc.* 121: 7124-7129.

Lieder CA, Brauman JI. 1974. Detection of neutral products in gas-phase, ion-molecule reactions. *J. Am. Chem. Soc.* 96: 4028-4030.

Lourderaj U, Sun R, Kohale SC, Barnes GL, de Jong WA, Windus TL, Hase WL. 2014. The VENUS/NWChem software package. Tight coupling between chemical dynamics simulations and electronic structure theory. *Comput. Phys. Commun.* 185(3): 1074-1080.

Mann DJ, Hase WL. 1998. Trajectory studies of S_N2 nucleophilic substitution. 6. translational activation of the $Cl^- + CH_3Cl$ reaction. *J. Phys. Chem. A* 102: 6208-6214.

Mensa-Bonsu G, Tozer DJ, Verlet JRR. 2019. Photoelectron spectroscopic study of $I^- \cdot ICF_3$: a frontside attack S_N2 pre-reaction complex. *Phys. Chem. Chem. Phys.* 21(26): 13977-13985.

Merkel A, Havlas Z, Zahradnik R. 1988. Evaluation of the rate-constant for the S_N2 reaction $CH_3F + H^- \rightarrow CH_4 + F^-$ in the gas-phase. *J. Am. Chem. Soc.* 110(25): 8355-8359.

Meyer J, Carrascosa E, Michaelsen T, Bastian B, Li A, Guo H, Wester R. 2019. Unexpected indirect dynamics in base-induced elimination. *J. Am. Chem. Soc.* 141: 20300-20308.

Meyer J, Wester R. 2017. Ion-molecule reaction dynamics. *Annu. Rev. Phys. Chem.* 68(1): 333-353.

Michaelsen T, Bastian B, Ayasli A, Strübin P, Meyer J, Wester R. 2020. The influence of vibrational excitation on the reaction of F^- with CH_3I: Spectator mode behavior, enhancement and suppression. *J. Phys. Chem. Lett.* 11: 4331-4336.

Michaelsen T, Bastian B, Strübin P, Meyer J, Wester R. 2020. Proton transfer dynamics modified by CH-stretching excitation. *Phys. Chem. Chem. Phys.* 22: 12382-12388.

Mikosch J, Frühling U, Trippel S, Schwalm D, Weidemüller M, Wester R. 2006. Velocity map imaging of ion-molecule reactive scattering: The $Ar^+ + N_2$ charge transfer reaction. *Phys. Chem. Chem. Phys.* 8: 2990-2999.

Mikosch J, Otto R, Trippel S, Eichhorn C, Weidemüller M, Wester R. 2008. Inverse temperature dependent lifetimes of transient S_N2 ion-dipole complexes. *J. Phys. Chem. A* 112: 10448-10452.

Mikosch J, Trippel S, Eichhorn C, Otto R, Lourderaj U, Zhang JX, Hase WL, Weidemüller M, Wester R. 2008. Imaging nucleophilic substitution dynamics. *Science* 319(5860): 183-186.

Mikosch J, Weidemüller M, Wester R. 2010. On the dynamics of chemical reactions of negative ions. *Int. Rev. Phys. Chem.* 29: 589-617.

Mikosch J, Zhang J, Trippel S, Eichhorn C, Otto R, Sun R, DeJong W, Weidemüller M, Hase WL, Wester R. 2013. Indirect dynamics in a highly exoergic substitution reaction. *J. Am. Chem. Soc.* 135(11): 4250-4259.

Neumark DM, Wodtke AM, Robinson GN, Hayden CC, Lee YT. 1985. Molecular-beam studies of the $F + H_2$ reaction. *J. Chem. Phys.* 82(7): 3045-3066.

Neumark DM, Wodtke AM, Robinson GN, Hayden CC, Shobatake K, Sparks RK, Schafer TP, Lee YT. 1985. Molecular-beam studies of the $F + D_2$ and F. HD reactions. *J. Chem. Phys.* 82(7): 3067-3077.

Olasz B, Czakó G. 2018. Mode-specific quasiclassical dynamics of the $F^- + CH_3I$ S_N2 and proton-transfer reactions. *J. Phys. Chem. A* 122(41): 8143-8151.

Olasz B, Szabó I, Czakó G. 2017. High-level ab initio potential energy surface and dynamics of the $F^- + CH_3I$ S_N2 and proton-transfer reactions. *Chem. Sci.* 8(4): 3164-3170.

Olmstead WN, Brauman JI. 1977. Gas-phase nucleophilic displacement reactions. *J. Am. Chem. Soc.* 99(13): 4219-4228.

Otto R, Brox J, Stei M, Trippel S, Best T, Wester R. 2012. Single solvent molecules can affect the dynamics of substitution reactions. *Nat. Chem.* 4(7): 534-538.

Otto R, Brox J, Trippel S, Stei M, Best T, Wester R. 2013. Exit channel dynamics in a micro-hydrated S_N2 reaction of the hydroxyl anion. *J. Phys. Chem. A* 117(34): 8139-8144.

Otto R, Xie J, Brox J, Trippel S, Stei M, Best T, Siebert MR, Hase WL, Wester R. 2012. Reaction dynamics of temperature-variable anion water clusters studied with crossed beams and by direct dynamics. *Faraday Discuss* 157: 41-57.

Palma J, Clary DC, et al. 2000. A quantum model hamiltonian to treat reactions of the type $X + YCZ_3 \rightarrow XY + CZ_3$: Application to $O(3P) + CH_4 \rightarrow OH + CH_3$. *J. Chem. Phys.* 112(4): 1859-1867.

Payzant JD, Tanaka K, Betowski LD, Bohme DK. 1976. Gas-phase S_N2 reactions at silicon and carbon centers - experimental appraisal of theory. *J. Am. Chem. Soc.* 98(4): 894-899.

Pei L, Carrascosa E, Yang N, Falcinelli S, Farrar JM. 2015. Velocity map imaging study of charge-transfer and proton-transfer reactions of CH_3 radicals with H_3^+. *J. Phys. Chem. Lett. 6*(9): 1684-1689.

Pei L, Farrar JM. 2012. Ion imaging study of reaction dynamics in the $N^+ + CH_4$ system. *J. Chem. Phys. 137*(15): 154312.

Polanyi JC. 1972. Some concepts in reaction dynamics. *Acc. Chem. Res. 5*(5): 161-168.

Qiu M, Ren Z, Che L, Dai D, Harich SA, Wang X, Yang X, Xu C, Xie D, Gustafsson M, Skodje RT, Sun Z, Zhang DH. 2006. Observation of feshbach resonances in the $F + H_2 \rightarrow HF + H$ reaction. *Science 311*: 1440.

Raugei S, Cardini G, Schettino V. 1999. An ab initio molecular dynamics study of the S_N2 reaction $Cl^- + CH_3Br \rightarrow CH_3Cl + Br^-$. *J. Chem. Phys 111*: 10887.

Raugei S, Cardini G, Schettino V. 2001. Microsolvation effect on chemical reactivity: The case of the $Cl^- + CH_3Br$ S_N2 reaction. *J. Chem. Phys. 114*(9): 4089-4098.

Regan CK, Craig SL, Brauman JI. 2002. Steric effects and solvent effects in ionic reactions. *Science 295*(5563): 2245-2247.

Reichert EL, Thurau G, Weishaar JC. 2002a. Nonstatistical translational energy distribution of H_2 elimination products from $Co^+(^3F_4)$. propane. *J. Phys. Chem. A 106*(23): 5563-5576.

Reichert EL, Thurau G, Weishaar JC. 2002b. Velocity map imaging of ion-molecule reaction products: $Co^+(^3F_4)$. isobutane. *J. Chem. Phys. 117*: 653.

Schiff HI, Bohme DK. 1975. Flowing afterglow studies at york university. *Int. J. Mass Spectrometry Ion Phys. 16*(1): 167-189.

Schlegel HB, Mislow K, Bernardi F, Bottoni A. 1977. Abinitio investigation into S_N2 reaction—frontside attack versus backside attack in reaction of F^- with CH_3F. *Theor. Chim. Acta. 44*(3): 245-256.

Schmatz S. 2004. Quantum dynamics of gas-phase S_N2 reactions. *ChemPhysChem. 5*(5): 600-617.

Shaik SS, Pross A. 1982. S_N2 reactivity of CH_3X derivatives - a valence bond approach. *J. Am. Chem. Soc. 104*(10): 2708-2719.

Sharma N, Biswas R, Lourderaj U. 2020. Dynamics of a gas-phase S_NAr reaction: Non-concerted mechanism despite the meisenheimer complex being a transition state. *Phys. Chem. Chem. Phys. 22*: 26562.

Stei M, Carrascosa E, Dörfler A, Meyer J, Olasz B, Czakó G, Li A, Guo H, Wester R. 2018. Stretching vibration is a spectator in nucleophilic substitution. *Sci. Adv. 47*(7): eaas9544.

Stei M, Carrascosa E, Kainz MA, Kelkar AH, Meyer J, Szabó I, Czakó G, Wester R. 2016. Influence of the leaving group on the dynamics of a gas-phase S_N2 reaction. *Nat. Chem. 8*(2): 151-156.

Su T, Chesnavich WJ. 1982. Application of the ion-polar molecule collision rate constant by trajectory calculations. *J. Chem. Phys. 76*: 5183.

Sun L, Song K, Hase WL. 2002. A S_N2 reaction that avoids its deep potential energy minimum. *Science. 296*(5569): 875-878.

Sun R, Davda CJ, Zhang J, Hase WL. 2015. Comparison of direct dynamics simulations with different electronic structure methods. $F^- + CH_3I$ with MP2 and DFT/B97-1. *Phys. Chem. Chem. Phys. 17*(4): 2589-2597.

Sun R, Xie J, Zhang J, Hase WL. 2015. The $F^- + CH_3I \rightarrow FCH_3 + I^-$ entrance channel potential energy surface comparison of electronic structure methods. *Int. J. Mass Spectrom. 377*: 222-227.

Swart M, Solà M, Bickelhaupt FM. 2007. Energy landscapes of nucleophilic substitution reactions: A comparison of density functional theory and coupled cluster methods. *J. Comput. Chem. 28*(9): 1551-1560.

Szabó, I., Csaszar AG, Czakó G. 2013. Dynamics of the $F^- + CH_3Cl \rightarrow Cl^- + CH_3F$ S_N2 reaction on a chemically accurate potential energy surface. *Chem. Sci. 4*(12): 4362-4370.

Szabó I, Czakó G. 2015. Revealing a double-inversion mechanism for the $F^- + CH_3Cl$ S_N2 reaction. *Nat. Commun. 6*: 5972.

Szabó I, Olasz B, Czakó G. 2017. Deciphering front-side complex formation in S_N2 reactions via dynamics mapping. *J. Phys. Chem. Lett. 8*(13): 2917-2923.

Tachikawa H. 2006. Direct ab initio molecular dynamics study on a microsolvated S_N2 reaction of $OH^-(H_2O)$ with CH_3Cl. *J. Chem. Phys. 125*(13): 133119.

Tachikawa H, Igarashi M. 1999. A direct ab-initio dynamics study on a gas phase S_N2 reaction $F^- + CH_3Cl \rightarrow CH_3F + Cl^-$: dynamics of near-collinear collision. *Chem. Phys. Lett. 303*(1-2): 81-86.

Tachikawa H, Igarashi M. 2006. Direct ab initio molecular dynamics study on a S_N2 reaction $OH^- + CH_3Cl \rightarrow CH_3OH + Cl^-$: Effect of non-zero impact parameter on the reaction dynamics. *Chem. Phys. 324*: 639-646.

Tanaka K, Mackay GI, Payzant JD, Bohme DK. 1976. Gas-phase reactions of anions with halogenated methanes at 297./-2 K. *Can. J. Chem. 54*(10): 1643-1659.

Thomsen DL, Reece JN, Nichols CM, Hammerum S, Bierbaum VM. 2013. Investigating the alpha-effect in gas-phase S_N2 reactions of microsolvated anions. *J. Am. Chem. Soc. 135*(41): 15508-15514.

Tonner DS, McMahon TB. 2000. Non-statistical effects in the gas phase S_N2 reaction. *J. Am. Chem. Soc. 122*(36): 8783-8784.

Trippel S, Stei M, Otto R, Hlavenka P, Mikosch J, Eichhorn C, Lourderarj U, Zhang JX, Hase WL, Weidemüller M, Wester R. 2009. Kinematically complete chemical reaction dynamics. *J. Phys. Conf. Ser. (ICPEAC 2009) 194*: 012046.

Tucker SC, Truhlar DG. 1990. A six-body potential energy surface for the S_N2 reaction Cl-(g). CH3Cl(g) and a variational transition-state-theory calculation of the rate constant. *J. Am. Chem. Soc. 112*: 3338-3347.

Uggerud E. 2017. The factors determining reactivity in nucleophilic substitution. *Adv. Phys. Org. Chem. 51*: 1-57.

Vande Linde SR, Hase WL. 1989. A direct mechanism for S_N2 nucleophilic-substitution enhanced by mode selective vibrational-excitation. *J. Am. Chem. Soc. 111*: 2349-2351.

Vande Linde SR, Hase WL. 1990a. Complete multidimensional analytic potential-energy surface for $Cl^- + CH_3Cl$ S_N2 nucleophilic-substitution. *J. Phys. Chem. 94*: 2778.

Vande Linde SR, Hase WL. 1990b. Non-RRKM kinetics in gas-phase S_N2 nucleophilic substitution. *J. Phys. Chem. 94*: 6148.

Vande Linde SR, Hase WL. 1990c. Trajectory studies of S_N2 nucleophilic-substitution. i. dynamics of $Cl^- + CH_3Cl$ reactive collisions. *J. Chem. Phys. 93*: 7962-7980.

Viggiano AA, Morris RA. 1996. Rotational and vibrational energy effects on ion-molecule reactivity as studied by the VT-SIFDT technique. *J. Phys. Chem. A 100*: 19227-19240.

Viggiano AA, Morris RA, Paschkewitz JS, Paulson JF. 1992. Kinetics of the gas-phase reactions of chloride anion, Cl^- with CH_3Br and CD_3Br: Experimental evidence for nonstatistical behavior? *J. Am. Chem. Soc. 114*(26): 10477-10482.

Walden P. 1896. Über die gegenseitige Umwandlung optischer Antipoden. *Ber. Dtsch. Chem. Ges. 29*: 133-138.

Wang Y, Song H, Szabó I, Czakó G, Guo H, Yang M. 2016. Mode-specific S_N2 reaction dynamics. *J. Phys. Chem. Lett. 7*(17): 3322-3327.

Wester R. 2009. Radiofrequency multipole traps: Tools for spectroscopy and dynamics of cold molecular ions. *J. Phys. B 42*(15): 154001.

Wester R. 2014. Velocity map imaging of ion-molecule reactions. *Phys. Chem. Chem. Phys. 16*: 396-405.

Wester R, Bragg AE, Davis AV, Neumark DM. 2003. Time-resolved study of the symmetric S_N2-reaction $I^- + CH_3I$. *J. Chem. Phys. 119*: 10032-10039.

Wladkowski BD, Brauman JI. 1992. Substitution versus elimination in gas-phase ionic reactions. *J. Am. Chem. Soc. 114*(26): 10643-10644.

Wladkowski BD, Brauman JI. 1993. Application of Marcus theory to gas-phase S_N2 reactions: Experimental support of the Marcus theory additivity postulate. *J. Phys. Chem. 97*: 13158.

Wolfe S, Mitchell DJ, Schlegel HB. 1982. Theoretical-studies of S_N2 transition-states—substituent effects. *Can. J. Chem. 60*(11): 1291-1294.

Xie J, Hase WL. 2016. Rethinking the S_N2 reaction. *Science 352*(6281): 32-33.

Xie J, Otto R, Mikosch J, Zhang J, Wester R, Hase WL. 2014. Identification of atomic-level mechanisms for gas-phase $X^- + CH_3Y$ S_N2 reactions by combined experiments and simulations. *Acc. Chem. Res. 47*(10): 2960-2969.

Xie J, Otto R, Wester R, Hase WL. 2015. Chemical dynamics simulations of the monohydrated $OH^-(H_2O) + CH_3I$ reaction. atomic-level mechanisms and comparison with experiment. *J. Chem. Phys. 142*(24): 244308.

Xie J, Sun R, Siebert M, Otto R, Wester R, Hase WL. 2013. Direct dynamics simulations of the product channels and atomistic mechanisms for the $OH^- + CH_3I$ reaction. comparison with experiment. *J. Phys. Chem. A 117*: 7162.

Xie J, Zhang J, Sun R, Wester R, Hase WL. 2019. Correlation between the velocity scattering angle and product relative translational energy for S_N2 reactions. comparison of experiments and direct dynamics simulations. *Int. J. Mass Spectrom. 438*: 115-123.

Zhang G-d, Guan L-c, Yan Z-f, Cheng M, Gao H 2021. A three-dimensional velocity-map imaging setup designed for crossed ion-molecule scattering studies. *Chin. J. Chem. Phys. 34*: 71.

Zhang J, Hase WL. 2010. Electronic structure theory study of the $F^- + CH_3I \rightarrow CH_3Cl + F^-$ potential energy surface. *J. Phys. Chem. A 114*(36): 9635-9643.

Zhang J, Lourderaj U, Addepalli SV, de Jong WA, Hase WL. 2009. Quantum chemical calculations of the $Cl^- + CH_3I \rightarrow CH_3Cl + I^-$ potential energy surface. *J. Phys. Chem. A 113*(10): 1976-1984.

Zhang J, Lourderaj U, Sun R, Mikosch J, Wester R, Hase WL. 2013. Simulation studies of the $Cl^- + CH_3I$ S_N2 nucleophilic substitution reaction: Comparison with ion imaging experiments. *J. Chem. Phys. 138*(11): 114309.

Zhang J, Mikosch J, Trippel S, Otto R, Weidemüller M, Wester R, Hase WL. 2010. $F^- + CH_3I \rightarrow FCH_3 + I^-$ reaction dynamics. nontraditional atomistic mechanisms and formation of a hydrogen-bonded complex. *J. Phys. Chem. Lett. 1*(18): 2747-2752.

Zhao XG, Tucker SC, Truhlar DG. 1991. Solvent and secondary kinetic isotope effects for the microhydrated S_N2 reaction of $Cl^-(H_2O)_n$ with CH_3Cl. *J. Am. Chem. Soc. 113*(3): 826-832.

AUTHOR BIOGRAPHY

Roland Wester studied physics at the Universities of Konstanz and Heidelberg. He received his PhD from the University of Heidelberg in 1999 for Coulomb explosion imaging experiments of molecular ions. He then worked for two years at the University of California in Berkeley on femtosecond spectroscopy. From 2003 to 2010 he carried out research on ultracold molecules and cold molecular ions at the University of Freiburg. Since 2010 he is full professor at the University of Innsbruck.